Author Manuscript

Author Manuscript

Author Manuscript

Author Manuscript

HHS Public Access

Author manuscript

J Am Chem Soc. Author manuscript; available in PMC 2024 February 05.

Published in final edited form as:

J Am Chem Soc. 2024 January 24; 146(3): 2054–2061. doi:10.1021/jacs.3c10941.

Improving protein expression, stability, and function with ProteinMPNN

Kiera H. Sumida[1,2], **Reyes Núñez-Franco**[3], **Indrek Kalvet**[2,4,5], **Samuel J. Pellock**[2,4], **Basile I. M. Wicky**[2,4], **Lukas F. Milles**[2,4], **Justas Dauparas**[2,4], **Jue Wang**[2,4], **Yakov Kipnis**[2,4,5], **Noel Jameson**[1], **Alex Kang**[2], **Joshmyn De La Cruz**[2], **Banumathi Sankaran**[6], **Asim K. Bera**[2,4], **Gonzalo Jiménez-Osés**[3,7], **David Baker**[2,4,5,*]

[1]Department of Chemistry, University of Washington, Seattle 98195, WA, USA.

[2]Institute for Protein Design, University of Washington, Seattle 98195, WA, USA.

[3]Center for Cooperative Research in Biosciences, Basque Research and Technology Alliance, Derio 48160, Spain.

[4]Department of Biochemistry, University of Washington, Seattle 98195, WA, USA.

[5]Howard Hughes Medical Institute, University of Washington, Seattle 98195, WA, USA.

[6]Berkeley Center for Structural Biology, Molecular Biophysics, and Integrated Bioimaging, Lawrence Berkeley Laboratory, Berkeley 94720, CA, USA.

[7]Ikerbasque, Basque Foundation for Science, Bilbao 48013, Spain.

Abstract

Natural proteins are highly optimized for function but are often difficult to produce at a scale suitable for biotechnological applications due to poor expression in heterologous systems, limited solubility, and sensitivity to temperature. Thus, a general method that improves the physical properties of native proteins while maintaining function could have wide utility for protein-based technologies. Here we show that the deep neural network ProteinMPNN together with evolutionary and structural information provides a route to increasing protein expression, stability, and function. For both myoglobin and tobacco etch virus (TEV) protease, we generated designs with improved expression, elevated melting temperatures, and improved function. For TEV protease, we identified multiple designs with improved catalytic activity as compared to the parent sequence and previously reported TEV variants. Our approach should be broadly useful for improving the expression, stability, and function of biotechnologically important proteins.

[*]**Corresponding Author David Baker** – Department of Biochemistry, University of Washington, WA, USA; dabaker@uw.edu.

Supporting Information

The Supporting Information is available free of charge on the ACS Publications website.

Supplementary materials contain computational and experimental methods, details of crystallographic data collection, sequences of designs, structural diversity of natural and designed myoglobin variants in Figure S1, *in silico* metrics of myoglobin designs grouped by method in Figure S2, raw thermostability, spectrophotometric, and activity data in Figures S3-S7, S9-S10A, raw data from Michaelis Menten fitting of TEV activity assays in Figures S8 and S10B, data from MD simulations in Figures S12-S13, sequence similarity analysis of myoglobin designs in Table S1, and mass spectrometry data for purified myoglobin designs in Table S2 (PDF). Coordinates for the crystal structure of design dnMb19 have been deposited to the PDB under accession code 8U5A.

The authors declare no competing financial interest.

Author Manuscript Author Manuscript Author Manuscript Author Manuscript

Graphical Abstract

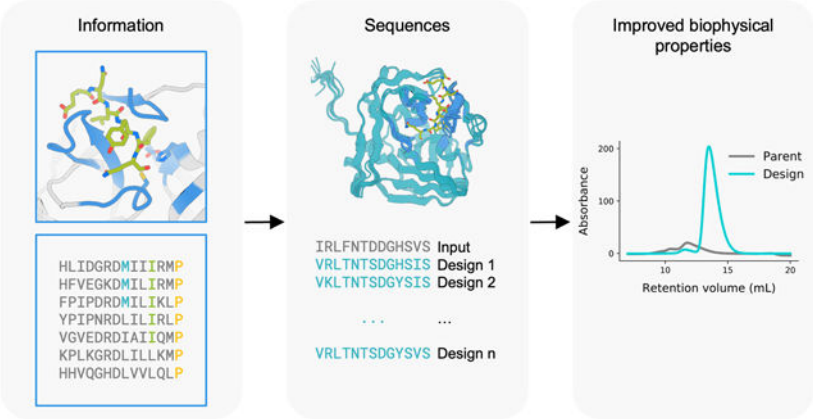

INTRODUCTION

Evolution has optimized function over stability in many natural proteins[1]; as a result, they often exhibit poor solubility, thermostability, and expression in heterologous systems, all of which reduce the yield of functional protein.[2,3] Many protein-based therapeutics and catalysts are limited in their industrial application by low stability, making protein stabilization a research area of increasing interest.[4,5] Experimental methods such as directed evolution have been extensively used to optimize desirable features in proteins, but are often prohibitively resource- and labor-intensive.[6,7] Subsequently, computational tools have been developed to achieve the benefits of directed evolution while minimizing experimental screening.[8-11] PROSS (protein repair one-stop shop), for example, utilizes evolutionary information and Rosetta physics-based energy calculations to perform sequence redesign using a three-dimensional (3D) structure as input, and has been shown to increase soluble expression and thermostability of several natural proteins.[8] More recently, advances in deep learning-based modeling of proteins have been applied to generate new variants of natural proteins, including language models that generate sequences for a given enzyme family or function[11], convolutional neural networks that leverage structural information for prediction of gain-of-function mutations[10], and shallow neural networks for guiding combinatorial directed evolution.[12]

Deep learning-based tools for protein sequence design have shown success in the generation of novel proteins with excellent expression, solubility, and sub-angstrom accuracy to design models.[11,13,14] ProteinMPNN generates highly stable sequences for designed backbones, and for native backbones, generates sequences that are predicted to fold to the intended structures more confidently than their native sequences.[13] We reasoned that ProteinMPNN could be applied to protein stability optimization and set out to develop a strategy for applying ProteinMPNN to natural proteins to increase solubility and stability. We chose as model systems one of the first proteins whose structure was solved, the oxygen storage protein myoglobin, and the widely used protease from tobacco etch virus (TEV).

Author Manuscript Author Manuscript Author Manuscript Author Manuscript

RESULTS

Protein stabilization with ProteinMPNN.

ProteinMPNN generates amino acid sequences that are predicted to fold to a given 3D structure. The method is purely structure-based and does not have access to functional information. Therefore, to retain protein function during sequence design, additional information must be provided to the network. We experimented with a range of approaches to retain functionality during the design process. In all targets, to preserve the catalytic machinery and substrate-binding site, we fixed the amino acid identities of the first shell functional positions – defined as those within 7 Å of the substrate in a ligand-bound crystal structure complex. In TEV protease, we used evolutionary information to further identify residues critical to activity. In myoglobin, we performed limited backbone redesign to further stabilize the structure. With the design space selected, we performed sequence design with ProteinMPNN, predicted the structures with AlphaFold2[15], and filtered by predicted local distance difference test score (pLDDT) and Cα root mean square deviation (RMSD) to the input structure (Figure 1).

Design of myoglobin variants with increased stability.

We first applied our design strategy to the model protein myoglobin. Myoglobin binds heme to carry oxygen in mammalian muscle tissue[16] and has relevance in clinical applications as a biomarker[17], as a versatile platform for biocatalytic applications[18-20], and in food science as an ingredient in artificial meat products[21-23]. Current efforts to create more stable variants of myoglobin have focused on the stabilization of the globin fold through stapling with cysteine-reactive noncanonical amino acids.[24,25]

We applied our ProteinMPNN design protocol described above using a crystal structure of human myoglobin, nMb (PDB: 3RGK)[26]. To preserve the oxygen storage function, we fixed the identities of 17 positions located around the heme ligand in the heme-bound structure (Figure 2A). 60 sequences were generated with ProteinMPNN and evaluated for their likelihood to recapitulate the myoglobin backbone coordinates using AlphaFold2 single-sequence predictions (see methods). Eight of the designs did so with high confidence (pLDDT > 85.0 and Cα RMSD < 1.0 Å; analogous single-sequence prediction of the native sequence yielded pLDDT = 50.6 and Cα RMSD = 7.5 Å). Four designs with close structural agreement in the heme-binding region were selected for experimental testing.

We also explored limited backbone redesign of poorly ordered regions to attempt to further stabilize the protein. The globin superfamily, of which myoglobin is a member, has a fold made up of eight alpha helical regions, with diversity in the termini and two loop regions flanking the heme-binding pocket[27-29] (Figure S1). We selected these less-conserved loop regions for backbone remodeling with RoseTTAFold joint inpainting (Figure 2A).[30] We generated two distinct sets of designs with structural remodeling: one with the region joining helices E and F redesigned, and one additionally including the CD-loop region (Figure 2A). From these remodeled backbones, we again performed sequence design with ProteinMPNN with the heme-binding site kept fixed as described above. Following filtering on structure

Author Manuscript Author Manuscript Author Manuscript Author Manuscript

prediction metrics (Figure S2), an additional 16 sequences were selected for experimental testing.

All 20 tested myoglobin designs have 41-55% sequence identity to the most similar protein (a myoglobin in all cases) in the UniRef100 database[31] (Table S1).

Synthetic genes encoding the designs and the parent sequence, nMb, were expressed in *E. coli*. The heme-loaded *holo*-proteins were purified via immobilized metal affinity chromatography (IMAC) and size exclusion chromatography (SEC). All designs expressed and were monomeric by SEC (Figure 2B). 13 of the 20 designs had higher levels (up to 4.1-fold increase) of total soluble protein yield (Figure 2C).

All 20 designs had similar heme-binding spectra to native myoglobin, with agreement in Soret maximum (407-413 nm vs 409 nm in native) and Q band features (500, 537, 582 and 630 nm), suggesting preservation of the native heme-binding mechanism (Figure S3).

The thermal stabilities of eight highly-expressing designs (six and two designed with and without backbone remodeling, respectively) were evaluated using circular dichroism (CD) spectroscopy. All eight designs had higher melting temperatures than native myoglobin, with six remaining fully folded at 95 °C (native myoglobin melts at 80 °C; Figures 2D and S4). Heme binding was also evaluated over a temperature gradient to determine functional thermal stability. All designs preserved heme binding at higher temperatures than native myoglobin (as monitored by changes to Soret band wavelength and intensity in the UV/Vis spectrum), with five designs maintaining significant heme-binding at 95 °C (Figure S5). One of the five designs, dnMb19, generated with the more aggressive backbone remodeling strategy, showed much higher thermal stability of heme binding compared to native myoglobin (Figure 2E). Overall, remodeling regions of the myoglobin backbone with inpainting increased the success rate for retaining heme-binding at elevated temperatures.

To understand the structural basis of these improvements in stability, we solved the crystal structure of dnMb19 (2.0 Å resolution, PDB: 8U5A). We found that it closely agreed with the AlphaFold2 prediction (0.66 Å Cα RMSD, Figure 2F), including the regions remodeled with inpainting. Native sidechain contacts with the heme group are largely preserved in dnMb19 (Figure 2G, inset I). Outside of the heme-binding site, the crystal structure confirms the structural changes introduced by inpainting: the C and E helices were elongated as designed and connected by a new loop (Figure 2G, inset II); the loop connecting the E and F helices has a new conformation, and the F helix was straightened through the replacement of PRO88 with GLU89 (Figure 2G, inset III). The Cα RMSD over the inpainted regions between the crystal structure and the AlphaFold2 model is 0.88 Å, with the largest deviation being in the CD-loop region (1.51 Å). These results illustrate the power of RoseTTAFold joint inpainting and ProteinMPNN to accurately remodel native protein backbones while increasing solubility, thermostability, and functional stability.

Design of TEV protease variants with improved stability and catalytic activity.

To explore the utility of ProteinMPNN sequence design for stabilizing enzymes, we next applied our design strategy to the cysteine protease from tobacco etch virus (TEV). TEV

Author Manuscript Author Manuscript Author Manuscript Author Manuscript

protease is widely used in biotechnological applications to specifically cleave between glutamine and serine in its recognition sequence (ENLYFQ/S) to remove purification tags from recombinant proteins. However, it is often difficult to use TEV protease due to its minimal soluble yield, low thermostability, and poor catalytic activity. These properties often necessitate long incubation times and result in incomplete cleavage.[32]

We applied our sequence design strategy to TEV protease starting from an autolysis-resistant S219D variant, TEVd (PDB: 1LVM)[33]. We defined the active site residues as described above to fix during redesign. We additionally fixed the amino acid identities of residues that are most conserved within the protein family (determined from a sequence alignment generated against UniRef30[31]), as residues distant from the active site can contribute significantly to function.[34] We ranked each amino acid identity at each position by degree of conservation in the sequence alignment and varied the percentage of these most highly conserved residues to fix during sequence redesign between 30-70%. We generated four distinct sets of designs that fixed the amino acid identities of just the active site residues, or the active site residues and 30%, 50%, and 70% of the most conserved residues in the TEV family (Figure 3A, see Methods). 144 sequences were generated with ProteinMPNN which were all predicted with high confidence to fold to the TEV structure by AlphaFold2 (pLDDT > 87.5; native TEV is predicted with pLDDT = 90) and possess 55% to 85% sequence identity to the parent sequence. All 144 designs were selected for experimental testing.

Synthetic genes encoding the designs, the parent sequence, TEVd, and several previously reported TEV variants were expressed in *E. coli*, and the resultant proteins were purified via IMAC and SEC. 134 of 144 designs expressed and were monomeric by SEC (Figure 3B). 129 of 144 designs exhibited higher levels of soluble expression than TEVd (TEVd average yield = 1 mg / L culture, designs average yield = 20.1 mg / L culture (Figure 3F)).

We evaluated catalytic activity using a previously described[7] coumarin derivative with 7-amino-4-trifluoromethylcoumarin conjugated to the C-terminus of the substrate peptide Ac-ENLYFQ (Figure S7A). Purified protein was incubated with the peptide-coumarin substrate, and 64 designs displayed progress curves with fluorescence above background, indicating substrate turnover (Figures S7B and S7C). Designs made with no evolutionary constraints had improved soluble expression over the parent but were not active on the peptide substrate, while designs with the highest activities were designed with the top 50% most conserved residues fixed (Figures 3F and 3G). We performed detailed kinetic analysis of three highly active designs from the 50% method – hyperTEV56, hyperTEV60, and hyperTEV89 – and the parent sequence TEVd[8]. The designs displayed improved catalytic efficiencies (k_{cat}/K_m) compared to TEVd, with up to 26-fold improvements (Table 1 and Figure S8).

Next, we tested the most active designs with a fusion protein substrate to assess performance on the target application of tag removal. The designs and a set of previously engineered TEV proteases[32,33,35-37] were incubated at 30 °C with the fusion protein substrate MBP-TEVcs-FKBP-EGFP, where MBP is maltose-binding protein, TEVcs is the TEV peptide cleavage site (ENLYFQS), FKBP is FK506-binding protein, and EGFP is enhanced green fluorescent protein. The extent of proteolysis was evaluated by monitoring the accumulation of cleaved product via sodium dodecyl sulfate-polyacrylamide gel electrophoresis (SDS-PAGE) (Figure

Author Manuscript Author Manuscript Author Manuscript Author Manuscript

S9). Two designs, hyperTEV56 and hyperTEV60, exhibited significantly higher rates of cleavage of protein substrate compared to the parent TEVd, yielding 50% cleaved product at ~4 hours of incubation while TEVd required 24 hours to reach an equivalent yield. The designs also outperformed other published TEV variants, with 30% turnover for superTEV, 15% turnover for TEV1Δ, and 50% turnover for S219V at 24 hours of incubation (Figures 3C and S10A). Straight-line fit of product accumulation and substrate depletion reveal catalytic efficiencies that corroborate those determined in the peptide assay (Figure S10B). The gains in catalytic efficiency are primarily due to increases in k_{cat}, which could reflect a higher fraction of enzyme in a catalytically competent state (see below).

Analysis by CD spectroscopy of TEVd and the most active design, hyperTEV60, indicated an approximate melting temperature of 84 °C for hyperTEV60, 40 °C higher than that of TEVd (Figures 3D and S11), and to our knowledge, higher than any previously described TEV variant. To further probe stability of the designed variant, TEVd and hyperTEV60 were incubated at 30 °C for various times and then used in the peptide-coumarin cleavage assay. After 4 hours of incubation, hyperTEV60 retained 90% of its original cleavage activity while TEVd was reduced to 15% of its original activity (Figure 3E), indicating a significant improvement in benchtop stability.

Given that catalytic and substrate-binding residues were kept fixed during design with ProteinMPNN, it is notable that significant improvements in k_{cat} were observed with both the peptide and protein substrates. Mutations distal to the active site can influence catalytic activity through stabilization of catalytically productive conformational states[38,39] or global conformational changes[40]. To investigate if stabilization of functional conformational states may be involved in activity enhancement, we performed microsecond molecular dynamics (MD) simulations on TEV-peptide complexes to probe the impact of the introduced mutations on overall protein dynamics. A general rigidification of loop regions distributed across the structure was observed in designs as compared to TEVd (Figure S12A). This backbone rigidification in distal regions not directly involved in substrate binding may be related to allosteric improvement of substrate binding as reflected by the 2- to 3-fold lower K_m values measured for the designed variants (Table 1). Rigidification in the region spanning residues 115 to 124 appeared to correlate with activity; the highest activity design, hyperTEV60, was most rigid, while TEVd and a design with no activity on the peptide substrate were most flexible in this region (Figure S12B). These trends were also observed in per-residue pLDDT analysis of AlphaFold2 ensemble predictions (Figure S12C). In all designs, we observed a decrease in the population of catalytically competent conformations of the Cys-His dyad ($d_{N\text{-}SH}$) compared to TEVd, but this shift was least significant in hyperTEV60, in agreement with its higher relative k_{cat} (Figure S13). These notable differences may begin to explain how ProteinMPNN enables substantial activity enhancements without explicit design elements to improve function. It is also possible that the major contribution to the increase in k_{cat} is from an increase in the fraction of the protein in the catalytically competent state more globally.

Author Manuscript Author Manuscript Author Manuscript Author Manuscript

DISCUSSION

We show that the expression, stability, and function of native proteins can be improved using ProteinMPNN guided by available sequence and structural information. For both TEV protease and human myoglobin, multiple variants were identified which showed higher soluble yield and thermostability than the native protein. The best of the TEV protease designs have higher apparent catalytic efficiency on peptide and protein substrates than the parent enzyme and previously reported variants. While the optimal number of residues to maintain (and perhaps enhance) function may have to be determined empirically for each case, the simplicity of our procedure and the compute efficiency and ease of use of ProteinMPNN make this straightforward, and the number of variants that need to be tested is far smaller than in typical experimental screens. We expect that our approach should be widely useful for improving the expression, stability, and function of biotechnologically important proteins.

Supplementary Material

Refer to Web version on PubMed Central for supplementary material.

ACKNOWLEDGMENTS

We thank A. Lauko, C. Norn, A. Roy, and L. Stewart for helpful discussions. We thank L. Goldschmidt and K. VanWormer for computational and experimental support, respectively. We thank X. Li and M. Lamb for analytical services. We also thank Agencia Estatal Investigacion of Spain (PID2021-125946OB-I00, CEX2021-001136-S, predoctoral fellowship; G.J.O., R.N.F.) for support of this work. Crystallographic data were collected at the Advanced Light Source (ALS), which is supported by the director, Office of Science, Office of 20 Basic Energy Sciences, and US Department of Energy under contract number DE-AC02-05CH11231. Funding was also provided by a National Science Foundation (NSF) grant CHE-1629214 (A.K.B.), the Air Force Office of Scientific Research FA9550-18-1-0297 (S.J.P.), a Defense Threat Reduction Agency grant HDTRA1-19-1-0003 (S.J.P.), the Bill and Melinda Gates Foundation grant OPP1156262 (A.K., J.C.), the National Institute of Health's National Institute of Allergy and Infectious Disease (R0AI160052, A.B.K.), the DARPA program Harnessing Enzymatic Activity for Lifesaving Remedies (HEALR) (HR0011-21-2-0012, A.K.B.), the Audacious Project at the Institute for Protein Design (L.F.M., A.K., J.C., E.B., A.K.B., D.B.), the Howard Hughes Medical institute (I.K., Y.K., D.B.), the Open Philanthropy Project Improving Protein Design Fund (K.H.S., S.J.P., I.K., B.I.M.W., J.D., J.W., Y.K., A.K., J.C., E.B., A.K.B., D.B.), Schmidt Futures (J.W.), a grant from the National Science Foundation (NSF) (DBI 1937533; D.B.), the Department of Energy ARPA-E Grant 2459-1671 (D.B.), an EMBO long-term fellowship (ALTF 139-2018; B.I.M.W.), a Washington Research Foundation Fellowship (S.J.P., J.W.), an Alfred P. Sloan Foundation Matter-to-Life Program Grant (G-2021-16899; D.B.), an EMBO Non-Stipendiary Fellowship (ALTF 1047-2019; L.F.M.), a Human Frontier Science Program Cross-Disciplinary Fellowship (LT000838/2018-C (I.K.), LT000395/2020-C (L.F.M.)), the National Institute of Health (R35 GM124773; N.J.) and a gift from Microsoft (J.D., D.B.).

REFERENCES

(1). Beadle BM; Shoichet BK Structural Bases of Stability–function Tradeoffs in Enzymes. J. Mol. Biol 2002, 321 (2), 285–296. [PubMed: 12144785]

(2). Magliery TJ Protein Stability: Computation, Sequence Statistics, and New Experimental Methods. Curr. Opin. Struct. Biol 2015, 33, 161–168. [PubMed: 26497286]

(3). Singh A; Upadhyay V; Upadhyay AK; Singh SM; Panda AK Protein Recovery from Inclusion Bodies of Escherichia Coli Using Mild Solubilization Process. Microb. Cell Fact 2015, 14, 41. [PubMed: 25889252]

(4). Thomson RES; Carrera-Pacheco SE; Gillam EMJ Engineering Functional Thermostable Proteins Using Ancestral Sequence Reconstruction. J. Biol. Chem 2022, 298 (10), 102435. [PubMed: 36041629]

Author Manuscript Author Manuscript Author Manuscript Author Manuscript

(5). Rathore N; Rajan RS Current Perspectives on Stability of Protein Drug Products during Formulation, Fill and Finish Operations. Biotechnol. Prog 2008, 24 (3), 504–514. [PubMed: 18484778]

(6). Cobb RE; Chao R; Zhao H Directed Evolution: Past, Present and Future. AIChE J. 2013, 59 (5), 1432–1440. [PubMed: 25733775]

(7). Arnold FH Directed Evolution: Bringing New Chemistry to Life. Angew. Chem. Int. Ed Engl 2018, 57 (16), 4143–4148. [PubMed: 29064156]

(8). Goldenzweig A; Goldsmith M; Hill SE; Gertman O; Laurino P; Ashani Y; Dym O; Unger T; Albeck S; Prilusky J; Lieberman RL; Aharoni A; Silman I; Sussman JL; Tawfik DS; Fleishman SJ Automated Structure- and Sequence-Based Design of Proteins for High Bacterial Expression and Stability. Mol. Cell 2018, 70 (2), 380. [PubMed: 29677494]

(9). Shroff R; Cole AW; Diaz DJ; Morrow BR; Donnell I; Annapareddy A; Gollihar J; Ellington AD; Thyer R Discovery of Novel Gain-of-Function Mutations Guided by Structure-Based Deep Learning. ACS Synth. Biol 2020, 9 (11), 2927–2935. [PubMed: 33064458]

(10). Lu H; Diaz DJ; Czarnecki NJ; Zhu C; Kim W; Shroff R; Acosta DJ; Alexander BR; Cole HO; Zhang Y; Lynd NA; Ellington AD; Alper HS Machine Learning-Aided Engineering of Hydrolases for PET Depolymerization. Nature 2022, 604 (7907), 662–667. [PubMed: 35478237]

(11). Madani A; Krause B; Greene ER; Subramanian S; Mohr BP; Holton JM; Olmos JL Jr; Xiong C; Sun ZZ; Socher R; Fraser JS; Naik N Large Language Models Generate Functional Protein Sequences across Diverse Families. Nat. Biotechnol 2023, 41, 1099–1106. [PubMed: 36702895]

(12). Wu Z; Kan SBJ; Lewis RD; Wittmann BJ; Arnold FH Machine Learning-Assisted Directed Protein Evolution with Combinatorial Libraries. Proc. Natl. Acad. Sci. U. S. A 2019, 116 (18), 8852–8858. [PubMed: 30979809]

(13). Dauparas J; Anishchenko I; Bennett N; Bai H; Ragotte RJ; Milles LF; Wicky BIM; Courbet A; de Haas RJ; Bethel N; Leung PJY; Huddy TF; Pellock S; Tischer D; Chan F; Koepnick B; Nguyen H; Kang A; Sankaran B; Bera AK; King NP; Baker D Robust Deep Learning–based Protein Sequence Design Using ProteinMPNN. Science 2022, 378 (6615), 49–56. [PubMed: 36108050]

(14). Wicky BIM; Milles LF; Courbet A; Ragotte RJ; Dauparas J; Kinfu E; Tipps S; Kibler RD; Baek M; DiMaio F; Li X; Carter L; Kang A; Nguyen H; Bera AK; Baker D Hallucinating Symmetric Protein Assemblies. Science 2022, 378 (6615), 56–61. [PubMed: 36108048]

(15). Jumper J; Evans R; Pritzel A; Green T; Figurnov M; Ronneberger O; Tunyasuvunakool K; Bates R; Žídek A; Potapenko A; Bridgland A; Meyer C; Kohl SAA; Ballard AJ; Cowie A; Romera-Paredes B; Nikolov S; Jain R; Adler J; Back T; Petersen S; Reiman D; Clancy E; Zielinski M; Steinegger M; Pacholska M; Berghammer T; Bodenstein S; Silver D; Vinyals O; Senior AW; Kavukcuoglu K; Kohli P; Hassabis D Highly Accurate Protein Structure Prediction with AlphaFold. Nature 2021, 596 (7873), 583–589. [PubMed: 34265844]

(16). Ordway GA; Garry DJ Myoglobin: An Essential Hemoprotein in Striated Muscle. J. Exp. Biol 2004, 207 (Pt 20), 3441–3446. [PubMed: 15339940]

(17). Hamm CW Cardiac Biomarkers for Rapid Evaluation of Chest Pain. Circulation 2001, 104 (13), 1454–1456. [PubMed: 11571234]

(18). Bordeaux M; Tyagi V; Fasan R Highly Diastereoselective and Enantioselective Olefin Cyclopropanation Using Engineered Myoglobin-Based Catalysts. Angew. Chem. Int. Ed Engl 2015, 54 (6), 1744–1748. [PubMed: 25538035]

(19). Carminati DM; Decaens J; Couve-Bonnaire S; Jubault P; Fasan R Biocatalytic Strategy for the Highly Stereoselective Synthesis of CHF2 -Containing Trisubstituted Cyclopropanes. Angew. Chem. Int. Ed Engl 2021, 60 (13), 7072–7076. [PubMed: 33337576]

(20). Brandenberg OF; Fasan R; Arnold FH Exploiting and Engineering Hemoproteins for Abiological Carbene and Nitrene Transfer Reactions. Curr. Opin. Biotechnol 2017, 47, 102–111. [PubMed: 28711855]

(21). Fraser R; Brown PO; Karr J; Holz-Schietinger C; Cohn E Methods and Compositions for Affecting the Flavor and Aroma Profile of Consumables. US Patent 9700067B2 2017.

Author Manuscript Author Manuscript Author Manuscript Author Manuscript

(22). Simsa R; Yuen J; Stout A; Rubio N; Fogelstrand P; Kaplan DL Extracellular Heme Proteins Influence Bovine Myosatellite Cell Proliferation and the Color of Cell-Based Meat. Foods 2019, 8 (10), 521. [PubMed: 31640291]

(23). Devaere J; De Winne A; Dewulf L; Fraeye I; Šoljić I; Lauwers E; de Jong A; Sanctorum H Improving the Aromatic Profile of Plant-Based Meat Alternatives: Effect of Myoglobin Addition on Volatiles. Foods 2022, 11 (13), 1985. [PubMed: 35804800]

(24). Moore EJ; Zorine D; Hansen WA; Khare SD; Fasan R Enzyme Stabilization via Computationally Guided Protein Stapling. Proc. Natl. Acad. Sci. U. S. A 2017, 114 (47), 12472–12477. [PubMed: 29109284]

(25). Iannuzzelli JA; Bacik J-P; Moore EJ; Shen Z; Irving EM; Vargas DA; Khare SD; Ando N; Fasan R Tuning Enzyme Thermostability via Computationally Guided Covalent Stapling and Structural Basis of Enhanced Stabilization. Biochemistry 2022, 61 (11), 1041–1054. [PubMed: 35612958]

(26). Hubbard SR; Hendrickson WA; Lambright DG; Boxer SG X-Ray Crystal Structure of a Recombinant Human Myoglobin Mutant at 2·8 Å Resolution. J. Mol. Biol 1990, 213 (2), 215–218. [PubMed: 2342104]

(27). Keppner A; Maric D; Correia M; Koay TW; Orlando IMC; Vinogradov SN; Hoogewijs D Lessons from the Post-Genomic Era: Globin Diversity beyond Oxygen Binding and Transport. Redox Biol 2020, 37, 101687. [PubMed: 32863222]

(28). Kapp OH; Moens L; Vanfleteren J; Trotman CN; Suzuki T; Vinogradov SN Alignment of 700 Globin Sequences: Extent of Amino Acid Substitution and Its Correlation with Variation in Volume. Protein Sci. 1995, 4 (10), 2179–2190. [PubMed: 8535255]

(29). Gell DA Structure and Function of Haemoglobins. Blood Cells Mol. Dis 2018, 70, 13–42. [PubMed: 29126700]

(30). Wang J; Lisanza S; Juergens D; Tischer D; Watson JL; Castro KM; Ragotte R; Saragovi A; Milles LF; Baek M; Anishchenko I; Yang W; Hicks DR; Expòsit M; Schlichthaerle T; Chun J-H; Dauparas J; Bennett N; Wicky BIM; Muenks A; DiMaio F; Correia B; Ovchinnikov S; Baker D Scaffolding Protein Functional Sites Using Deep Learning. Science 2022, 377 (6604), 387–394. [PubMed: 35862514]

(31). Suzek BE; Huang H; McGarvey P; Mazumder R; Wu CH UniRef: Comprehensive and Non-Redundant UniProt Reference Clusters. Bioinformatics 2007, 23 (10), 1282–1288. [PubMed: 17379688]

(32). Blommel PG; Fox BG A Combined Approach to Improving Large-Scale Production of Tobacco Etch Virus Protease. Protein Expr. Purif 2007, 55 (1), 53–68. [PubMed: 17543538]

(33). Phan J; Zdanov A; Evdokimov AG; Tropea JE; Peters HK 3rd; Kapust RB; Li M; Wlodawer A; Waugh DS Structural Basis for the Substrate Specificity of Tobacco Etch Virus Protease. J. Biol. Chem 2002, 277 (52), 50564–50572. [PubMed: 12377789]

(34). Halabi N; Rivoire O; Leibler S; Ranganathan R Protein Sectors: Evolutionary Units of Three-Dimensional Structure. Cell 2009, 138 (4), 774–786. [PubMed: 19703402]

(35). Kapust RB; Tözsér J; Fox JD; Anderson DE; Cherry S; Copeland TD; Waugh DS Tobacco Etch Virus Protease: Mechanism of Autolysis and Rational Design of Stable Mutants with Wild-Type Catalytic Proficiency. Protein Eng. 2001, 14 (12), 993–1000. [PubMed: 11809930]

(36). Sanchez MI; Ting AY Directed Evolution Improves the Catalytic Efficiency of TEV Protease. Nat. Methods 2020, 17 (2), 167–174. [PubMed: 31819267]

(37). Correnti CE; Gewe MM; Mehlin C; Bandaranayake AD; Johnsen WA; Rupert PB; Brusniak M-Y; Clarke M; Burke SE; De Van Der Schueren W; Pilat K; Turnbaugh SM; May D; Watson A; Chan MK; Bahl CD; Olson JM; Strong RK Screening, Large-Scale Production and Structure-Based Classification of Cystine-Dense Peptides. Nat. Struct. Mol. Biol 2018, 25 (3), 270–278. [PubMed: 29483648]

(38). Otten R; Pádua RAP; Bunzel HA; Nguyen V; Pitsawong W; Patterson M; Sui S; Perry SL; Cohen AE; Hilvert D; Kern D How Directed Evolution Reshapes the Energy Landscape in an Enzyme to Boost Catalysis. Science 2020, 370 (6523), 1442–1446. [PubMed: 33214289]

(39). Jiménez-Osés G; Osuna S; Gao X; Sawaya MR; Gilson L; Collier SJ; Huisman GW; Yeates TO; Tang Y; Houk KN The Role of Distant Mutations and Allosteric Regulation on LovD Active Site Dynamics. Nat. Chem. Biol 2014, 10 (6), 431–436. [PubMed: 24727900]

Author Manuscript Author Manuscript Author Manuscript Author Manuscript

(40). Ishida T. Effects of Point Mutation on Enzymatic Activity: Correlation between Protein Electronic Structure and Motion in Chorismate Mutase Reaction. J. Am. Chem. Soc 2010, 132 (20), 7104–7118. [PubMed: 20426479]

Author Manuscript Author Manuscript Author Manuscript Author Manuscript

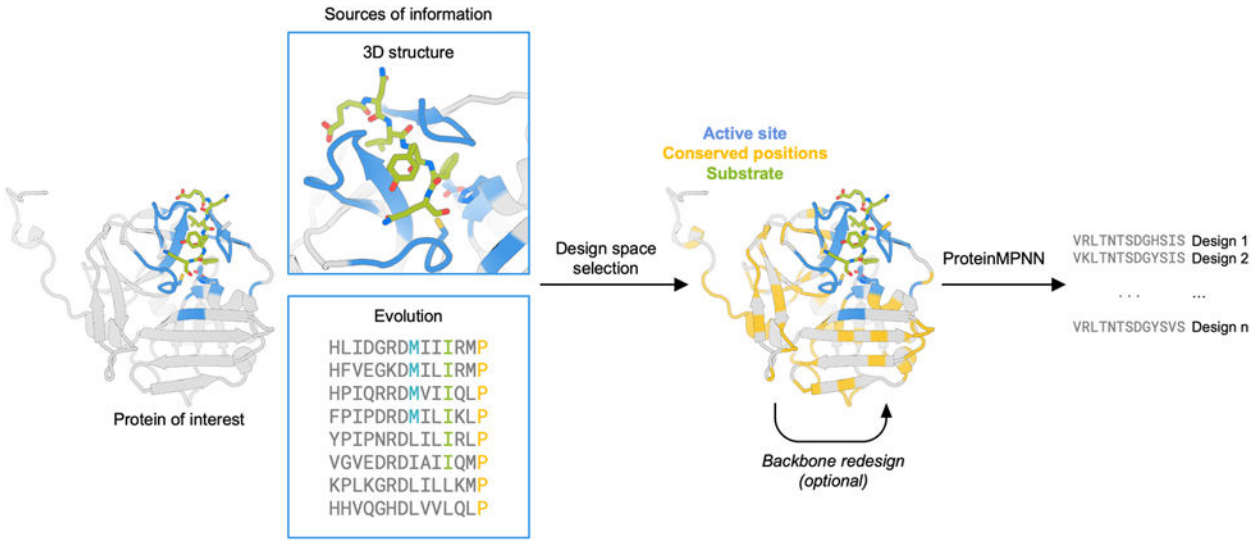

Figure 1.

Design strategy for optimization of protein expression and stability using ProteinMPNN. The design space is chosen to preserve native protein function by fixing the amino acid identities of residues close to the ligand and those that are highly conserved in multiple sequence alignments. The protein backbone structure and fixed position information of amino acids are input into ProteinMPNN, which generates new amino acid sequences likely to fold to the input structure. The backbone structure in loop regions can optionally be remodeled using RoseTTAfold joint inpainting to further idealize the input protein.

Author Manuscript Author Manuscript Author Manuscript Author Manuscript

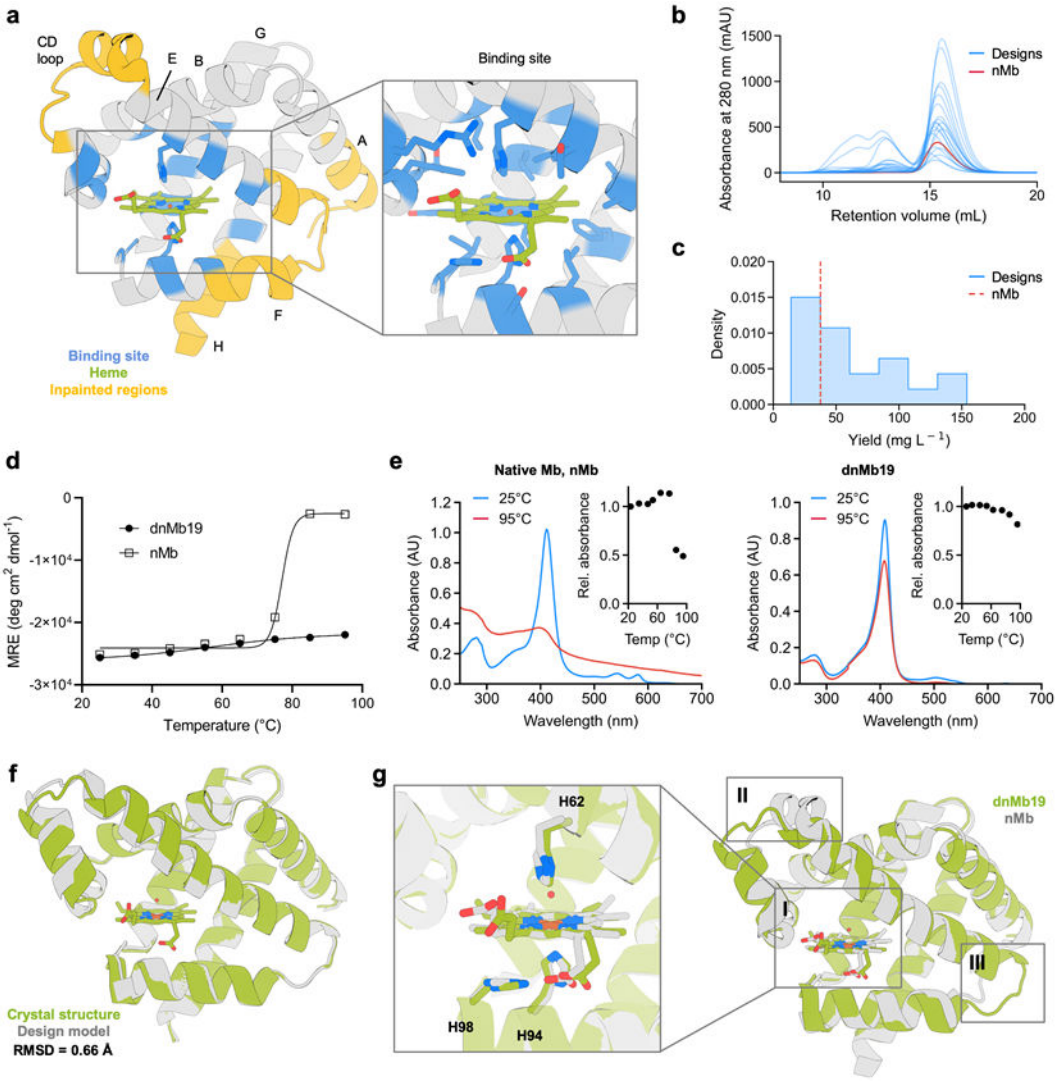

Figure 2.

ProteinMPNN design improves myoglobin expression and thermostability. (A) Positions adjacent to the heme were kept fixed during sequence design (shown in blue). Non-conserved regions (in yellow) were subjected to backbone remodeling. Inset shows the heme-binding site. (B) SEC traces of 20 designed myoglobin variants. (C) Soluble yield of myoglobin designs and native myoglobin nMb (represented as a red dashed line). (D) CD melting temperature plots of dnMb19 compared to native myoglobin (signal reported in molar residue ellipticity (MRE)). (E) Absorbance plots of dnMb19 and native myoglobin (inset shows temperature scan). (F) Structural alignment of the crystal structure (green) and AlphaFold2 (AF2) prediction (gray) of dnMb19. (G) Overlay of the crystal structure of native myoglobin (gray) and the crystal structure of dnMb19 (green, PDB: 8U5A). Non-conserved regions displayed in insets II and III were subjected to backbone redesign.

Author Manuscript Author Manuscript Author Manuscript Author Manuscript

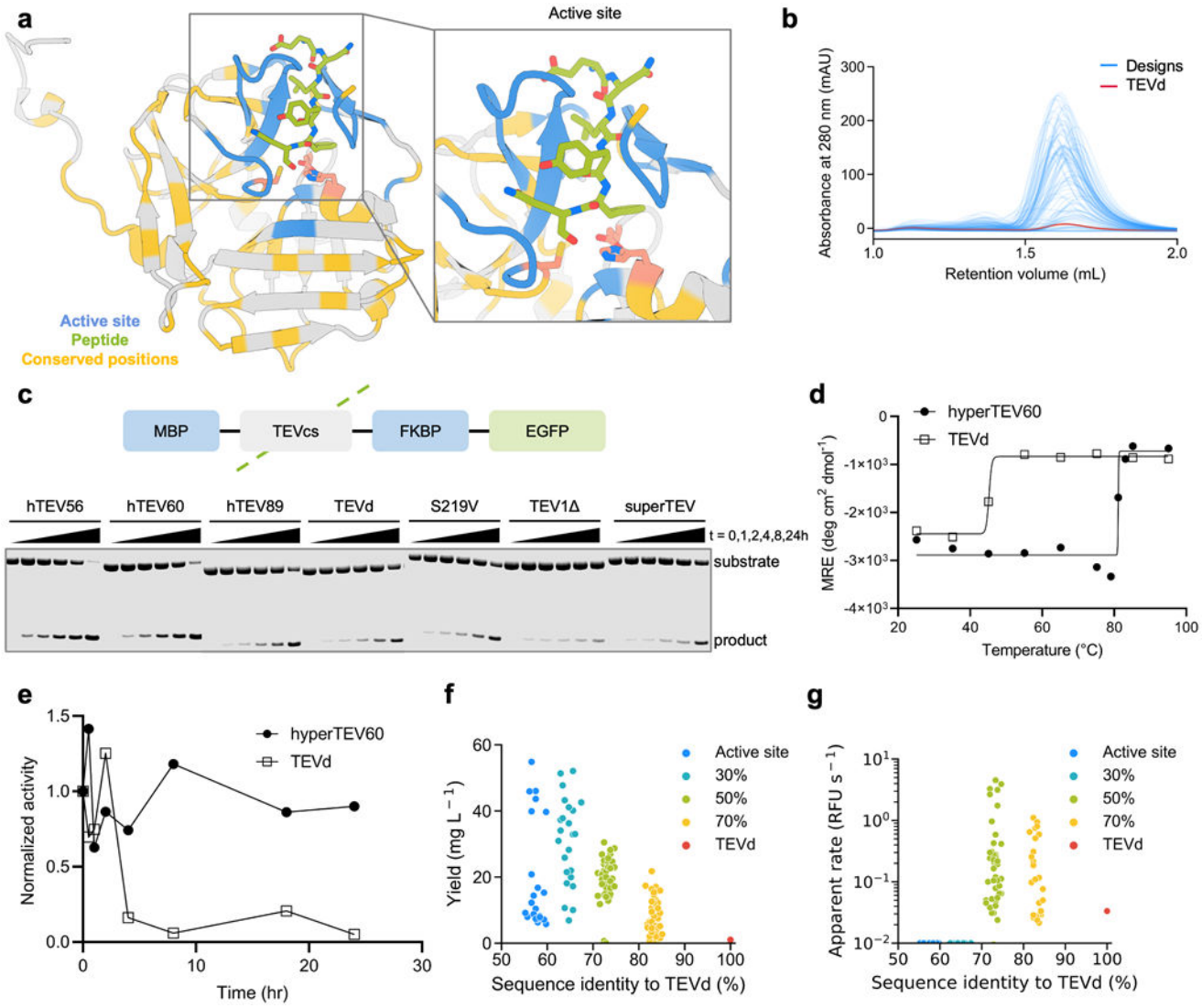

Figure 3.

ProteinMPNN sequence design improves TEV protease expression, thermostability, and catalytic efficiency. (A) TEVd (PDB: 1LVM) input structure with positions fixed during redesign highlighted. Active site residues surrounding the substrate (blue), 50% most highly conserved residues (yellow), and catalytic residues (pink) are highlighted. Inset shows zoom-in of the active site region. (B) SEC traces of designed TEV variants. (C) Diagram of TEV substrate (top) and fluorescent gel image of TEV cleavage reactions at various time points (bottom). (D) CD melting temperature plots of designed and native TEV (signal reported in molar residue ellipticity (MRE)). (E) Benchtop stability comparison of native TEVd and designed variant assessed as activity measured over time incubated at 30 °C before inclusion in assay. (F) Decreased evolutionary constraints correlate with higher soluble expression levels. Legend indicates regions fixed during design (all designs have active site fixed). (G) Designs made with the active site and 50% most conserved

residues fixed during design exhibited highest catalytic activity. Raw apparent rate reported in relative fluorescence units (RFU) per second.

Author Manuscript Author Manuscript Author Manuscript Author Manuscript

Author Manuscript Author Manuscript Author Manuscript Author Manuscript

Table 1.

Kinetic parameters for TEV redesigns and parent TEV variant.

Variant	k_{cat} (min^{-1})	K_m (μM)	k_{cat}/K_m (μM^{-1} min^{-1})	Fold-improvement in k_{cat}/K_m over parent
hyperTEV56	0.0106 ± 0.0005	1.4 ± 0.2	0.0077	20
hyperTEV60	0.014 ± 0.002	1.4 ± 0.4	0.01	26
hyperTEV89	0.0050 ± 0.0001	2 ± 1	0.0024	6.2
TEVd	0.0023 ± 0.0003	6 ± 3	0.00039	